Journal of the European Ceramic Society xxx (2016) xxx–xxx

Contents lists available at www.sciencedirect.com

Journal of the European Ceramic Society

journal homepage: www.elsevier.com/locate/jeurceramsoc

Solubility of tungsten in zirconium diboride solid solution

Ali Khadimallah [a,*], Xiaobao Li [b], KennethW. White [a]

[a] Department of Mechanical Engineering, University of Houston, Houston, TX, USA
[b] School of Civil Engineering, Hefei University of Technology, Anhui, China

ARTICLE INFO

Article history:
Received 15 February 2016
Received in revised form
23 November 2016
Accepted 25 November 2016
Available online xxx

Keywords:
ZrB_2
WC
Solubility of W in ZrB_2
Thermodynamic modeling
DFT
Gibbs free energy of WB_2

ABSTRACT

Zirconium diboride (ZrB_2) is arguably one of the most important ceramic materials for applications involving extreme high temperatures and oxidizing environments such as those encountered in re-entry vehicles and hypersonic aircraft, among others. Accordingly, enhancing the creep resistance of ZrB_2 is of critical importance. A viable approach to achieve the latter is through the addition of substitutional atoms such as tungsten. In this work, using a combination of quantum mechanics based first-principles simulations and thermodynamic modeling; we present the essential elements of the W-ZrB_2 phase diagram to enable the design of enhanced creep-resistant ultra-high temperature ZrB_2-alloys. In the course of the assessment, we estimate the Gibbs free energy of WB_2, nonexistent in the literature to date, and based on the developed phase diagram, conclude that the solubility of tungsten in ZrB_2 does not occur below ~1380 °C and that temperatures above ~1700 °C are needed to dissolve 1 mol% of W in ZrB_2.

1. Introduction

Transition metal diborides namely, ZrB_2 and HfB_2 have been classified as UHTCs for their unique characteristics such as thermal shock and oxidation resistance and high melting temperatures exceeding 3000 °C [1,2]. ZrB_2 has the advantage of lower density (~6.1 g cm^{-3}) compared to HfB_2 (~11.2 g cm^{-3}) with similar modulus and electrical conductivity [1]. These particular properties make ZrB_2 a potential candidate for aerospace applications [3] and other applications including hypersonic aircraft, thermocouple protection tubes and cutting tools [4,5]. Particularly, Sharp leading edges of atmospheric re-entry vehicles require advanced high temperature deformation resistance under oxidizing conditions.

Few experimental studies of the high-temperature deformation behavior of ZrB_2 based materials exist in the literature [6–12]. Accordingly, creep-related mechanisms are not well understood for these systems. However, recent work predicated on high-resolution electron backscatter imaging and indentation mapping analysis [13,14], has shown that 'mantle' dislocation flow accommodating a grain boundary sliding dominated creep governs ZrB_2-20% SiC deformation at 1800 °C. Accordingly, one objective of the present paper is to explore the solubility of minor alloy additions such as W in ZrB_2 solid solution system, however, the details associated with W solid solution on our mechanical model to inhibit the creep accommodation mechanism within grain boundary networks has been presented elsewhere [14,15], and remains the subject of a manuscript currently in preparation.

Our preliminary four-point bending creep experiments show at least half an order of magnitude decrease in the strain rates with 1.5 mol% W dissolved in ZrB_2 lattice in comparison with ZrB_2-20% SiC. The parallel behavior found by Kats et al. [16] for 4–6 mol% solutions of WC resulted in reduced creep rates of ZrC alloys by an order of magnitude, while higher WC concentrations resulted in lowering melting temperatures and depreciating the high-temperature creep resistance.

Further advantages associated with the addition of WC to ZrB_2 include the improved sintering of the diboride. Presence of oxides on ZrB_2 grain surfaces (mainly ZrO_2 and B_2O_3) prevents shrinkage and promotes grain coarsening. WC decomposes ZrO_2 to produce ZrC and W which subsequently dissolve in the ZrB_2 lattice [17]. A 98% final relative density of the pressureless sintered ZrB_2-WC mixture was reached after 540 min at 2150 °C [17]. Additionally, reduced oxygen weight gain and oxide scale thickness reduction was observed in WC containing ZrB_2 materials after exposure to oxidizing atmosphere at 1600 °C. It was shown that amounts of less than 8 mol% of WC improve the oxidation resistance of ZrB_2 by liquid phase sintering of the porous ZrO_2 surface layer [18,19].

For all the reasons mentioned above, ZrB_2-WC systems seem to be potential candidates for improved high temperature appli-

* Corresponding author.
E-mail addresses: akhadimallah@uh.edu, ali.khadimallah@yahoo.fr (A. Khadimallah).

http://dx.doi.org/10.1016/j.jeurceramsoc.2016.11.039
0955-2219/

cations. Specifically, W content in ZrB_2 will dictate the creep resistance behavior of the alloy and an understanding of the solubility of WC in ZrB_2 is necessary for the alloy development. Scattered ternary and binary phase diagrams (Zr-W-B [20–22], Zr-W-C [23], Zr-B-C [24], W-B-C [25], Zr-B [24], Zr-C [24], B-C [24], W-B [26], W-C [27] and Zr-W [28]) exist in the literature. Unfortunately, the 4-component phase diagram (Zr-W-B-C) has not been published to date. However, due to the strong influence of W on ZrB_2 creep behavior, it is important to evaluate its solubility. In the present manuscript, Density Functional Theory (DFT) and thermodynamic modeling, combined with data from the literature, are used to assess W content in ZrB_2 solid solution with temperature based on a sublattice description of the solution phase. Four pressureless sintered ZrB_2-based materials are also examined to highlight some particular microstructural features associated with different sintering temperatures.

The outline of the paper is as follows: in Section 2, we describe the general processing procedure of the alloys. Characterization results that provide details on the different microstructures are presented in Section 3. Our general approach to combine experimental data from the literature, thermodynamic modeling and quantum mechanical simulations to assess the solubility of W in ZrB_2 is discussed in Section 4 and finally we conclude with a brief summary in Section 5.

2. Experimental procedure

ZrB_2 (Grade A, H.C. Starck, Newton, MA, USA), WC (Grade DS-60, H.C. Starck, Newton, MA, USA) and B_4C (Grade HS, H.C. Starck, Germany) powders were used in this study. Powders were attrition milled (Model 01-HD, Union Process, Akron, OH, USA) for 4 h at 600 rpm, in Isopropyl alcohol, at 1:1 solvent to powder ratio, using Cobalt-bonded WC media. The mixture was dried using a 300 rpm stir hot plate at ~100 °C. After lightly grinding the dried powder with a pestle and mortar, a 50-mesh sieve separated the large particles. The mixed powders were first uniaxially pressed at 30 MPa for 60 s into 4.5cm × 2.5cm × 1.5 cm billets followed by cold isostatic pressing at 180 MPa for 180 s. We introduced the green compacts into a graphite vacuum furnace (Centorr Vacuum Industries, Nashua, NH, USA) and rested on a Grafoil sheet (GrafTech, Inc). Theoretical density was calculated based on the rule of mixture, green density was measured from the mass and the volume of the compact and final density was measured using Archimedes' method where the immersing fluid is water. All heating cycles were achieved under mild vacuum (~100 mTorr) up to 1650 °C, at a 10 °C/min heating rate. The furnace chamber was then backfilled with 99.999% Argon until the end of the cycle and naturally cooled to room temperature. Powder heat treatment was performed in effort to enhance densification behavior of ZrB_2 as in [29]. Processing information is summarized in Table 1.

3. Results and microstructure

Final densities of samples 1–4 were all higher than 98% of the theoretical densities (Table 2). Heat-treated powders showed a ~2% enhancement in the final density due possibly to a decrease in the oxygen content initially present on the powder surface and generated during the milling process. Similar increase (~3%) in the final density was obtained for ZrB_2 powders heat treated in Argon atmosphere at 1150 °C for 8 h after Spark Plasma Sintering for temperatures between 1650 °C and 1900 °C [29]. Hydrogen reduction was attempted with sample 1 with the aim of reducing oxygen content of the powder prior to sintering to enhance its densification behavior. In fact, some of the metal oxides associated with the current powders can be reduced to pure metals in the presence of Hydrogen. Pure W can be obtained from WO_3 on WC surfaces, at temperatures less then 1000 °C in Hydrogen atmosphere through successive reduction reactions [30]. On the other hand, Hydrogen showed less effectiveness in reducing ZrO_2 even at much higher temperatures [31]. It is unclear whether the ~2% density enhancement observed between samples 1 and 2 is due to hydrogen reduction reactions or simply the evaporation of liquid oxides; this determination must follow a more thorough examination.

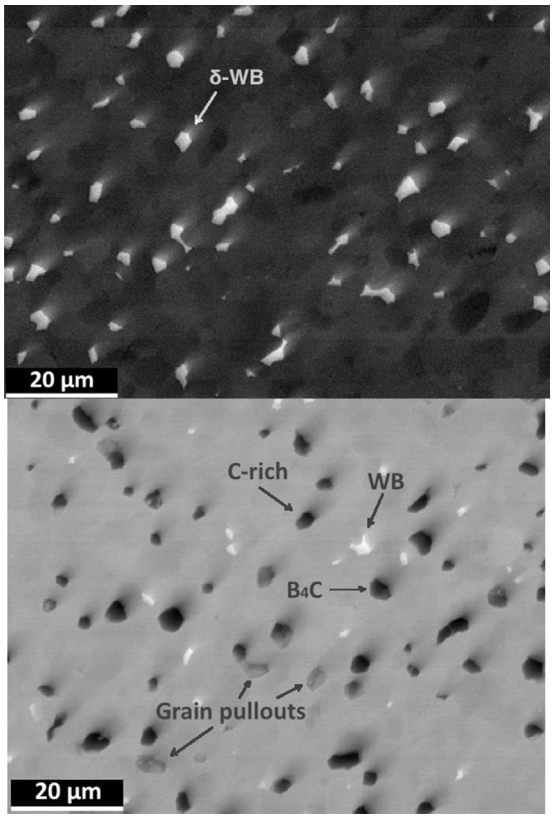

Fig. 1. Backscattered electron SEM image of polished surfaces from sample 3 (top) and 1 (bottom).

Microstructures of the samples sintered at the same temperature exhibited similar features. The 2100 °C samples presented a two-phase microstructure whereas two extra phases appeared in the 1975 °C samples (See Fig. 1). Only ZrB_2 was detected on the X-ray diffractometer in samples 1 and 2 due to the low concentration of the other phases. Chemical analysis using EDS revealed the presence of WB, unreacted B_4C and carbon rich (B-C phase in Table 2) phases. In contrast, both ZrB_2 and WB patterns appeared for samples 3 and 4 (Fig. 2). Comparable grain sizes were obtained for the specimens sintered at the same temperatures with ~1.7 μm grain growth in those subjected to 2100 °C during sintering. Presence of WB and B-C phases in the 1975 °C and WB in the 2100 °C samples in different amounts and sizes could have contributed dissimilarly to the reduction of grain growth. Also, carbon was shown to reduce ZrB_2 grain growth by reducing grain boundary mobility [32]. Therefore, the difference in grain sizes between the two sets of microstructures (high and low temperatures) can be attributed to high temperature soaking period of samples 3 and 4 at the high temperature and possibly to the difference in carbon and secondary phases volume fractions present in the two microstructures.

Solid solution formation in ZrB_2 was confirmed by the shift in XRD peaks towards higher 2θ angles, indicating the dissolution of W-C in ZrB_2. A decrease of the lattice parameter was observed consistently with W (~135 pm) substituting Zr (~160 pm) and C

Please cite this article in press as: A. Khadimallah, et al., Solubility of tungsten in zirconium diboride solid solution, *J Eur Ceram Soc* (2016), http://dx.doi.org/10.1016/j.jeurceramsoc.2016.11.039